460

Egypt. J. Chem. **Vol. 66**, No. 10 pp. 93 - 106 (2023)

Synthesis of New 1,2,3-Triazole-Based Compounds of Potential Anti-Breast Cancer Activity Targeting Aromatase Enzyme Inhibition

Yasmin M. Syam[1*], Radwan El-Haggar[2], Manal M. Anwar[1], Alaa H. Hashim[2], Ola Nosseir[2], Wafaa A. Zaghary[2]

[1]*Department of Therapeutic Chemistry, National Research Centre, Dokki, Cairo 12622, Egypt*
[2]*Department of Pharmaceutical Chemistry, Faculty of Pharmacy, Helwan University, Ain Helwan, 11795, Cairo, Egypt*

Abstract

Depriving the estrogen in the body by inhibiting the aromatase enzyme is thought to be one of the most effective pathways for preventing and treating breast cancer. This study deals with the synthesis of new derivatives bearing a 4-bromophenyl-5-methyl-1,2,3-triazole scaffold hybridized with various heterocyclic rings of reported aromatase inhibition activity such as pyridine, pyrimidine, and pyrazole 4-14, aiming to gain new potent antiproliferative molecules against breast cancer via inhibition of the aromatase enzyme. The cytotoxic activity of the target compounds was evaluated against breast cancer (MCF-7) as well as the normal cell line (WI-38). The derivatives 5b, 5c and 10 were the most promising analogues with a high safety margin against WI38. The latter derivatives were also assessed as aromatase inhibitors and were also subjected to molecular docking studies to determine their potential.

1. Introduction

Breast cancer is one of the most major causes of death in women across all age categories around the world. It is considered as the second cause of death in women after the lung cancer. About 6.27 million breast cancer-related fatalities were recorded by the World Health Organization in 2021 [1-4]. Around 75% of patients have hormone-responsive breast cancer [5]. Due to the production of estrogen in peripheral tissues in postmenopausal women, the risk of breast cancer is continuing to rise, whereas strogen production is primarily controlled by the ovaries in premenopausal women [6-8].

Estrogens (estradiol and estrone) are formed from androgens (androstenedione and testosterone) through demethylation and aromatization processes, which are catalyzed by the rate limiting enzyme aromatase (CYP19) [9]. Estrogens are crucial in encouraging the proliferation of neoplastic breast epithelial cells in breast cancer patients with positive estrogen receptors through signaling estrogen receptor-mediated pathways. As a result, patients with breast cancer of the hormone-dependent kind have been found to have an increased risk of metastasis and recurrence when their estrogen levels are high [10-12].

Aromatase is a monooxygenase heme protein belonging to the P450 family. It is a microsomal enzyme complex made up of two primary components: flavoprotein (NADPH) nicotinamide adenine dinucleotide phosphate-cytochrome P450 reductase and hemoprotein CYP19 (family of cytochrome P450). Aromatase (CYP19) is responsible for the conversion of androgens to estrogens [13-15]. Numerous tissues, including the ovary, placenta, bone, adipose, testis, skin, and brain, have been discovered to contain aromatase [16]. It has been proved that breast cancer tissues express aromatase and make more estrogen than non-cancerous cells. This is one of the key causes of

aromatase's high level of attention as a significant breast cancer treatment [17].

There are two primary methods for slowing down, managing, and controlling the progression of hormone-dependent breast cancers: binding estrogen receptors with ERAs (like tamoxifen) or preventing estrogen production with aromatase inhibitors (AIs) [18]. Tamoxifen acts as a selective estrogen receptor modulator producing excellent successful treatment of both early and advanced breast cancer. The occurrence of resistance and a number of draw back side effects impacted the therapeutic efficacy of the latter drug [19-21]. On the other hand, aromatase suppressors constitute a novel approach to endocrine therapy that is based on the inhibition of estrogen production, which is relevant for the aromatase activity [22,23]. Numerous studies have classified aromatase inhibitors into two types. Steroidal AIs, such as exemestane and formestane, constitute the first class and they act irreversibly to suppress the aromatase enzyme, whereas non-steroidal AIs are the second class which act by coordinating the heme iron in the catalytic site of aromatase leading to a reversible inhibition. Aminoglutethimide is considered the first-generation aromatase inhibitor to treat breast cancer [26]. Fadrozole and rogletimide constitute the second-generation, while letrozole, vorozole, and anastrozole are the third-generation AI which reversibly inhibit aromatase enzyme (Fig. 1) [27-29].
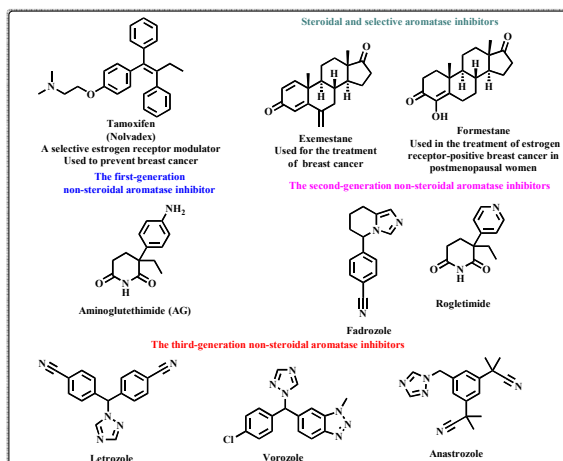

Fig. 1: The molecular structures of the most commonly prescribed drugs for the treatment of hormone-dependent breast cancer

Despite the fact that all currently available, whether steroidal or nonsteroidal, show positive clinical results, long-term use of them can result in the development of drug resistance as well as serious side effects like osteoporosis, cardiovascular disease, fractured bones, and muscular and joint pain [1,30].

Therefore, the need to explore novel AIs is still necessary to develop new drugs with better pharmacokinetic properties.

It has been reported that 1,2,3-triazole-based compounds are stable and can interact with various biological targets via the generation of hydrogen bonds, dipole-dipole interactions, and π--stacking interactions, which facilitate the creation of stable complexes, triggering a series of metabolic activations resulting in a wide spectrum of biological activities [31-34]. From extensive molecular docking studies, it has been found that the task of the triazole ring is coordination of triazole nitrogen lone pair of electrons with the Fe^{3+} in center of the heme moiety in the active site of the enzyme, leading to potent AI [35-37].

El-Naggar *et al*. reported that the 1,2,3-triazole derivative I and its ester analogue II were potent aromatase inhibitors with IC_{50} values, 0.00015 and 0.00074 µM in comparison to anastrozole as a reference drug (IC_{50} value, 0.00241 µM) [38] (Fig. 2). Also, the Touaibia group exhibited that the dicyanodiphenylmethyl-1,2,3-trizole analogue III of letrozole showed equipotent activity to letrozole with an IC_{50} value of 0.008 µM whereas the 1,4-disubstituted-1,2,3-triazole IV represented an IC_{50} value of 1.36 µM [39].

In addition, different studies showed that the triazolobenzene sulfonamide analogue V and the 1,2,3-triazolylbenzoxazole derivative VI revealed promising aromatase suppression potency with IC_{50} values; 0.20 and 0.26 µM, respectively. The molecular docking study of V represented hydrogen interactions with Met374 and Ser478, which were expected to be the most important amino acid residues for aromatase suppression [40] (Fig. 2).

Also, James McNulty *et al*. have published the 1,2,3-triazole acetate derivative VII and its alcohol analogue VIII as having potent selective AI activity with potencies as low as 50 nM [41] (Fig. 2).
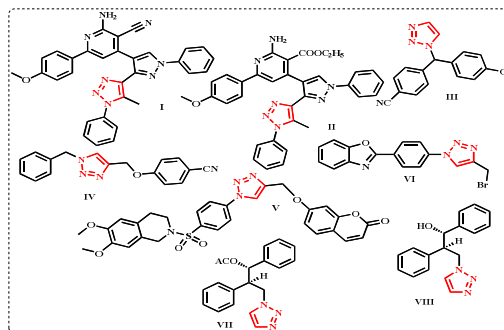

Fig. 2: A variety of 1,2,3-triazole-based analogues with strong aromatase inhibition activity

Based on the synergistic effect that is usually gained due to the molecular hybridization aspect and in the search for novel aromatase inhibitors, the current study focused on the design and synthesis of new derivatives having the 4-bromophenyl-5-methyl-1,2,3-triazole scaffold conjugated with various hetero-atomic nuclei of reported aromatase inhibition activity, such as pyridine [42], pyrimidine [43], and pyrazole [44], with the goal of receiving new potent anti-proliferative agents against breast cancer via aromatase enzyme inhibition (Fig. 3). It has been expected that the 4-bromophenyl moiety could enhance the binding of the 1,2,3-triazole derivatives via hydrophobic interactions with the active site of the target enzyme. In addition, it was intended to conjugate the parent scaffold with sulfonamide groups such as compounds 14 and 15, aiming to produce extra hydrogen bonding with the active site, leading to more aromatase inhibition activity (Fig. 3). All final compounds were subjected to the MTT assay to evaluate their cytotoxic activity. The aromatase suppression activity was assessed for the most potent cytotoxic candidates. In addition, a molecular docking study was carried out for the most promising compounds to explore their modes of interaction with the target enzyme.
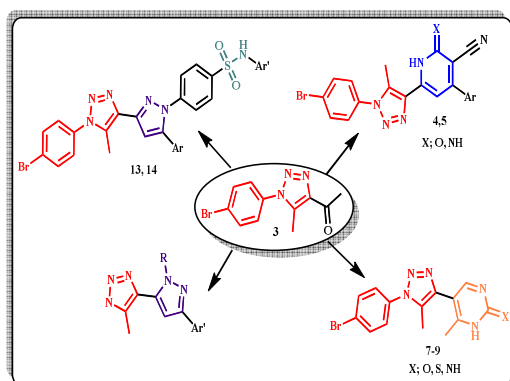

Fig. 3: The design strategy of the new 4-bromophenyl-5-methyl-1,2,3-triazole-based compounds

1. Materials and methods
1.1. Chemistry

The melting points were measured using an Electrothermal IA 9000 series digital melting point instrument (Electrothermal, Essex, UK) in open glass capillaries. The results are uncorrected. Shimadzu FT-IR 8201 PC spectrophotometer was used to measure the infrared (IR) spectra in KBr pellets. On a JEOL-500MHz spectrometer, the ^1H and ^{13}C NMR spectra were recorded in DMSO, and the chemical shifts were recorded in δ values relative to TMS. Mass spectra were recorded on a GC-MS QP1000 EX

Shimadzu. Elemental analyses were performed using ElmenterVaru EL Germany Instrument.

2.1.1. 1-(1-(4-Bromophenyl)-5-methyl-1H-1,2,3-triazol-4-yl)ethan-1-one (3)
The compound **3** was prepared according to reported method (45, 46), yield: 78%; mp: 120-122 °C.

2.1.2. General procedure for the preparation of 6-(1-(4-bromophenyl)-5-methyl-1H-1,2,3-triazol-4-yl)-4-substituted aryl-2-oxo-1,2-dihydropyridine-3-carbonitrile 4a-c

A mixture of the acetyl triazole derivative **3** (2.80 g, 10 mmol), ethyl cyanoacetate (1.13 g, 10 mmol) and the appropriate aldehydes namely; *p*-tolyl, *p*-methoxy, *N,N* dimethyl amino benzaldehyde (10 mmol) in the presence of ammonium acetate (6.16 g, 80 mmol) in butanol (50 mL) was heated under reflux for 6h. The solid separated upon cooling was filtered and crystallized from acetic acid to obtain the desired product **4a-c**, respectively.

2.1.2.1. 6-(1-(4-Bromophenyl)-5-methyl-1H-1,2,3-triazol-4-yl)-2-oxo-4-(p-tolyl)-1,2-dihydropyridine-3-carbonitrile (4a)
Yield (71%); mp: 243-245°C; IR (KBr, cm^{-1}): 3428 (NH), 3100 (CH, aromatic), 2919 (CH-aliphatic), 2217 (CN), 1650 (C=O); 1H NMR (DMSO-d_6, δ ppm): 2.40, 2.63 (2s, 6H, 2CH$_3$), 6.75 (s, 1H, pyridine-H3), 7.28-7.45, 7.67-7.80 (2m, 8H, Ar-H), 10.38 (s, 1H, NH, exchangeable with D$_2$O); MS, m/z (%): 448 [M.$^+$+2] (23.76), 446 [M.$^+$] (20.21); Analysis for C$_{22}$H$_{16}$BrN$_5$O (446.31); Calcd.: %C, 59.21; H, 3.61; N, 15.69; Found: %C, 59.07; H, 3.87; N, 16.49.

2.1.2.2. 6-(1-(4-Bromophenyl)-5-methyl-1H-1,2,3-triazol-4-yl)-4-(4-methoxyphenyl)-2-oxo-1,2-dihydropyridine-3-carbonitrile (4b)
Yield (74%); mp: 295-297°C; IR (KBr, cm^{-1}): 3435 (NH), 3095 (CH, aromatic), 2923 (CH-aliphatic), 2216 (CN), 1650 (C=O); ^1H NMR (DMSO-d_6, δ ppm): 2.60 (s, 3H, CH$_3$), 3.83 (s, 3H, OCH3), 6.83 (s, 1H, pyridine-H3), 7.13, 7.62, 7.71, 7.87 (4d, 8H, Ar-H), 12.59 (s, 1H, NH, exchangeable with D$_2$O); ^{13}C NMR (DMSO-d_6, δ ppm): 10.75 (CH$_3$), 55.86 (OCH$_3$), 114.76 (CN), 118.38, 121.47, 124.09, 127.86, 128.10, 130.26, 133.26, 134.90, 139.55, 141.26, 143.60, 148.90, 152.20, 155.09 (aromatic-C), 160.38 (C=O); MS, m/z (%): 464 [M.$^+$+2] (15.09), 462 [M.$^+$] (17.84); Analysis for C$_{22}$H$_{16}$BrN$_5$O$_2$ (462.31); Calcd.: %C, 57.16; H, 3.49; N,15.15. Found: %C, 57.38; H, 3.64; N, 15.27.

2.1.2.3. 6-(1-(4-Bromophenyl)-5-methyl-1H-1,2,3-triazol-4-yl)-4-(4-(dimethylamino)phenyl)-2-oxo-1,2-dihydropyridine-3-carbonitrile (4c)

_____

Yield (78%); mp: 250-252°C; IR (KBr, cm^{-1}): 3425 (NH), 3120 (CH, aromatic), 2918 (CH-aliphatic), 2213 (CN), 1650 (C=O); ^{1}H NMR (DMSO-d6, δ ppm): 2.29, 3.02 (2s, 9H, 3CH$_3$), 6.75-6.92 (m, 3H, Ar-H), 7.64 (d, 2H, Ar-H), 7.76-7.88 (m, 4H, Ar-H), 8.35 (s, 1H, NH, exchangeable with D$_2$O); 13C NMR (DMSO-d$_6$, δ ppm): 10.70 (CH$_3$), 41.53 (-N(CH$_3$)2), 114.15 (CN), 118.94, 120.26, 123.42, 125.27, 127.84, 129.97, 133.22, 133.30, 135.24, 138.28, 141.28, 142.43, 149.32, 152.27, 155.21 (aromatic-C), 168.02 (C=O); MS, m/z (%): 477 [M.$^{+}$+2] (25.16), 475 [M.$^{+}$] (29.74); Analysis for C$_{23}$H$_{19}$BrN$_6$O (475.35); Calcd.: %C, 58.12; H, 4.03; N, 17.68; Found: %C, 57.87; H, 3.92; N, 17.73.

2.1.3. General procedure for the preparation of 6-(1-(4-bromophenyl)-5-methyl-1H-1,2,3-triazol-4-yl)-2-imino-4-substituted aryl-1,2-dihydropyridine-3-carbonitrile 5a-c

A mixture of acetyl 1,2,3-triazole derivative 3 (2.80 g, 10 mmol), malononitrile (0.66 g, 10 mmol), ammonium acetate (6.16 g, 80 mmol), and the appropriate aldehydes, namely p-tolyl, p-methoxy, and N,N-dimethylamino benzaldehyde (10 mmol) in butanol (50 mL) was refluxed for 6 hours. The solid separated upon cooling was filtered and crystallized from ethanol to obtain the desired products 5a-c, respectively.

2.1.3.1. 6-(1-(4-Bromophenyl)-5-methyl-1H-1,2,3-triazol-4-yl)-2-imino-4-(p-tolyl)-1,2-dihydropyridine-3-carbonitrile (5a)

Yield (69%); mp: 170-172°C; IR (KBr, cm^{-1}): 3433, 4325 (2NH), 3090 (CH, aromatic), 2920 (CH-aliphatic), 2200 (CN), 1596 (C=N); ^{1}H NMR (DMSO-d$_6$, δ ppm): 2.40, 2.62 (2s, 6H, 2CH$_3$), 6.85-7.03 (m, 4H, Ar-H), 7.53-7.69 (m, 5H, Ar-H), 8.90, 9.27 (2s, 2H, 2NH, exchangeable with D$_2$O); MS, m/z (%): 446 [M.$^{+}$+2] (24.95), 444 [M.$^{+}$] (22.86); Analysis for C$_{22}$H$_{17}$BrN$_6$ (445.32); Calcd.: %C, 59.34; H, 3.85; N,18.87; Found: %C, 59.57; H, 3.73; N, 18.63.

2.1.3.2. 6-(4-Bromophenyl)-5-methyl-1H-1,2,3-triazol-4-yl)-2-imino-4-(4-methoxyphenyl)-1,2-dihydropyridine-3-carbonitrile (5b)

Yield (75%); mp: 165-167°C; IR (KBr, cm^{-1}): 3432, 4330 (2NH), 3089 (CH, aromatic), 2922 (CH-aliphatic), 2207 (CN), 1600 (C=N). ^{1}H NMR (DMSO-d$_6$, δ ppm): 2.47 (s, 3H, CH3), 3.83 (s, 3H, OCH3), 6.95 (s, 1H, pyridine-H5), 7.60, 7.67 (2d, 4H, Ar-H), 7.69-7.73 (m, 4H, Ar-H), 8.67, 9.27 (2s, 2H, 2NH, exchangeable with D$_2$O); ^{13}C NMR (DMSO-d6, δ ppm): 10.06 (CH3), 56.58 (OCH$_3$), 116.02 (CN), 120.27, 121.38, 123.84, 127.58, 127.90, 129.85, 131.36, 133.23, 133.39, 138.42, 140.38,

141.29, 144.63, 152.64, 154.87 (aromatic-C); MS, m/z (%): 463 [M.$^{+}$+2] (26.06), 461 [M.$^{+}$] (23.75); Analysis for C$_{22}$H$_{17}$BrN$_6$O (461.32); Calcd.: %C, 57.28; H, 3.71; N,18.22; Found: %C, 57.57; H, 3.73; N, 18.63.

2.1.3.3. 6-(1-(4-Bromophenyl)-5-methyl-1H-1,2,3-triazol-4-yl)-4-(4-(dimethylamino)phenyl)-2-imino-1,2-dihydropyridine-3-carbonitrile (5c)

Yield (90%); mp: 149-151°C; IR (KBr, cm^{-1}): 3427, 3422 (2NH), 3086 (CH, aromatic), 2918 (CH-aliphatic), 2205 (CN), 1602 (C=N). ^{1}H NMR (DMSO-d$_6$, δ ppm): 2.40, 3.01 (2s, 9H, 3CH$_3$), 6.85-7.65 (m, 6H, Ar-H), 7.85-7.97 (m, 3H, Ar-H), 8.30, 10.26 (2s, 2H, 2NH, exchangeable with D$_2$O); MS, m/z (%): 476 [M.$^{+}$+2] (18.93), 474 [M.$^{+}$] (20.63); Analysis for C$_{23}$H$_{20}$BrN$_7$ (474.37); Calcd.: %C, 58.24; H, 4.25; N, 20.67; Found: %C, 58.52; H, 4.36; N, 20.52.

2.1.4. 1-(1-(4-Bromophenyl)-5-methyl-1H-1,2,3-triazol-4-yl)butane-1,3-dione (6)

A mixture of the acetyl triazole derivative 3 (2.80 g, 10 mmol) and Na metal (1.15 g, 5 mmole) in ethyl acetate (10 mL) was heated under reflux for 6 hrs. The solid separated upon cooling was filtered and crystallized from ethanol to afford the intermediate diketone product 7.

Yield (65%), mp: 207-209°C, IR (KBr, cm^{-1}): 3063 (CH, aromatic), 2965 (CH-aliphatic), 1721, 1684 (2C=O); ^{1}H NMR (DMSO-d$_6$, δ ppm): 2.30 (s, 3H, CH$_3$), 2.40 (s, 3H, CH$_3$), 3.87 (s, 2H, CH$_2$), 7.54-7.60 (m, 4H, Ar-H); ^{13}C NMR (DMSO-d$_6$, δ ppm): 10.06 (CH$_3$), 32.16 (CO-CH$_3$), 52.61 (COCH$_2$), 110.13, 123.11, 129.50, 134.53, 135.34, 140.5, 131.23 (aromatic-C), 170.41 (2C=O); MS, m/z (%): 324 [M.$^{+}$+2] (28.06), 322 [M.$^{+}$] (25.05); Analysis for C$_{13}$H$_{12}$BrN$_3$O$_2$ (322.16); Calcd.: %C, 48.47; H,3.75; N, 13.04; Found: %C, 48.63; H, 3.90; N,12.85.

2.1.5. General procedure for the preparation of 5-(1-(4-bromophenyl)-5-methyl-1H-1,2,3-triazol-4-yl)-6-methylpyrimidin-2(1H)-one, thione or imine derivatives (7-9)

A mixture of the diketone derivative 6 (3.24 g, 10 mmol) and an equimolar amount of urea, thiourea, and/or guanidine HCl (10 mmol) in the presence of conc. sulfuric acid (0.5 mL) was refluxed in absolute ethanol (40 mL) for 6 hrs. The reaction mixture was cooled, poured onto ice/water. The formed precipitate was filtered and crystallized from absolute ethanol to give the corresponding compounds 7–9.

2.1.6. 5-(1-(4-bromophenyl)-5-methyl-1H-1,2,3-triazol-4-yl)-6-methylpyrimidin-2(1H)-one (7)

_____

Yield (81%), mp: 201-203°C; IR (KBr, cm^{-1}): 3327 (NH), 3060 (CH, aromatic), 2965 (CH-aliphatic), 1678 (C=O); ^{1}H NMR (DMSO-d$_6$, δ ppm): 2.24, 2.39 (2s, 6H, 2CH3), 6.71 (s, 1H, pyrimidine-H4), 7.64-7.90 (m, 4H, Ar-H), 9.82 (s, 1H, NH, exchangeable with D$_2$O); ^{13}C NMR (DMSO-d$_6$, δ ppm): 9.76 (CH$_3$), 15.59 (CH$_3$), 110.51, 123.27, 129.38, 131.84, 134.58, 135.70, 140.90, 153.29 (aromatic-C), 164.87 (C=O); MS, m/z (%): 346 [M.$^+$+2] (30.07), 344 [M.$^+$] (29.27); Analysis for C$_{14}$H$_{12}$BrN$_5$O (346.19), Calcd.: %C, 48.57; H, 3.49; N, 20.23; Found: %C, 48.83; H, 3.62; N, 20.42.

2.1.7. 5-(1-(4-Bromophenyl)-5-methyl-1H-1,2,3-triazol-4-yl)-6-methylpyrimidine-2(1H)-thione (8)

Yield (77%), mp: 210-212°C; IR (KBr, cm^{-1}): 3320 (NH), 3065 (CH, aromatic), 2970 (CH-aliphatic); ^{1}H NMR (DMSO-d6, δ ppm): 2.16, 2.34 (2s, 6H, 2CH$_3$), 6.61 (s, 1H, pyrimidine-H4), 6.80-7.62 (m, 4H, Ar-H), 9.85 (s, 1H, NH, exchangeable with D$_2$O); MS, m/z (%): 364 [M.$^+$+2] (23.27), 362 [M.$^+$] (22.08).; Analysis for C$_{14}$H$_{12}$BrN$_5$S (362.25); Calcd.: %C, 46.42; H, 3.34; N, 19.33; S, 8.85; Found: %C, 46.63; H, 3.58; N, 19.50; S, 8.72.

2.1.8. 5-(1-(4-Bromophenyl)-5-methyl-1H-1,2,3-triazol-4-yl)-6-methylpyrimidin-2(1H)-imine (9)

Yield (69%); mp: 198-201°C; IR (KBr, cm^{-1}): 3347 (NH), 3103 (CH, aromatic), 2985 (CH-aliphatic), 1594 (C=N); ^{1}H NMR (DMSO-d$_6$, δ ppm): 2.16, 2.29 (2s, 6H, 2CH$_3$), 6.63 (s, 1H, NH, exchangeable with D$_2$O), 7.21-7.88 (m, 5H, Ar-H), 9.50 (s, 1H, NH, exchangeable with D$_2$O); MS, m/z (%): 347 [M.$^+$+2] (26.38), 345 [M.$^+$] (24.23); Analysis for C$_{14}$H$_{13}$BrN$_6$ (345.20); Calcd.: %C, 48.71; H, 3.80; N, 24.35; Found: %C, 48.82; H, 3.94; N, 24.57.

2.1.9. 1-(4-bromophenyl)-5-methyl-4-(3-methyl-1-phenyl-1H-pyrazol-5-yl)-1H-1,2,3-triazole (10)

A mixture of the diketone derivative 6 (3.24 g, 10 mmol) and an equimolar amount of phenyl hydrazine (10 mmol, 1.08 mL) in the presence of conc. sulfuric acid (0.5 mL) was refluxed in absolute ethanol (40 mL) for 6 hrs. The reaction mixture was cooled, poured onto ice/water. The precipitate formed upon cooling was filtered and crystallized from isopropanol to give the pyrazole derivative 10.
Yield (66%), mp: 188-190°C; IR (KBr, cm^{-1}): 3086 (CH, aromatic), 2979 (CH-aliphatic), 1595 (C=N). ^{1}H NMR (DMSO-d$_6$, δ ppm): 2.16, 2.41 (2s, 6H, 2CH3), 6.55 (s, 1H, Pyrazole-H), 7.33-7.39 (m, 5H, Ar-H), 7.57, 7.81 (2d, 4H, Ar-H); ^{13}C NMR (DMSO-d$_6$, δ ppm): 9.31, 13.77 (2CH3), 109.61 (pyrazole-C4), 123.31, 124.65, 127.39, 127.58, 129.33, 129.72, 133.18, 133.43, 135.38, 136.24, 140.35, 149.22 (aromatic-C); MS, m/z (%): 396 [M.$^+$+2] (25.09), 394 [M.$^+$] (26.45); Analysis for C$_{19}$H$_{16}$BrN$_5$ (394.28); Calcd.: %C, 57.88; H, 4.09; N, 17.76.; Found: %C, 57.92; H, 3.98; N, 17.85.

2.1.10. General procedure for the preparation of 1-(1-(4-bromophenyl)-5-methyl-1H-1,2,3-triazol-4-yl)-3-aryl-prop-2-en-1-one (11a-e)

A mixture of the acetyl derivative 3 (2.80 g, 10 mmol) and the appropriate aldehydes, namely, benzaldehyde, p-anisaldehyde, p-N,N-dimethylamino benzaldehyde, 5-bromovanillin, and veratraldehyde (10 mmol) in 5% ethanolic sodium hydroxide solution (40 mL) was stirred at room temperature overnight. The reaction mixture was poured onto ice/water and neutralized with dil. HCl. The formed precipitate was filtered and crystallized from absolute ethanol to give the corresponding chalcone compounds 11a-e.

2.1.10.1. 1-(1-(4-Bromophenyl)-5-methyl-1H-1,2,3-triazol-4-yl)-3-phenylprop-2-en-1-one (11a)

Yield (82%); mp: 240-242°C; IR (KBr, cm^{-1}): 3062 (CH, aromatic), 2922 (CH-aliphatic), 1661 (C=O); ^{1}H NMR (DMSO-d$_6$, δ ppm): 2.40 (s, 3H, CH$_3$), 7.45 (dd, 1H, -CO-CH=CH), 7.62-7.63 (m, 4H, Ar-H), 7.81-7.84 (m, 5H, Ar-H), 7.86 (dd, 1H, -CO-CH=CH); ^{13}C NMR (DMSO-d$_6$, δ ppm): 9.92 (CH$_3$), 104.51, 117.27, 117.74 (aromatic-C), 124.71 (-CO-CH=CH), 126.41, 127.08, 128.33, 132.78, 134.36, 139.82 (aromatic-C), 142.05 (-CO-CH=CH), 144.86, 150.32, 158.39, 158.85 (aromatic-C), 191.71 (C=O); MS, m/z (%): 370 [M.$^+$+2] (24.60), 368 [M.$^+$] (19.05); Analysis for C$_{18}$H$_{14}$BrN$_3$O (368.23); Calcd.: %C, 58.71; H, 3.83; N,11.41; Found: %C, 58.43; H, 3.62; N, 11.62.

2.1.10.2. 1-(1-(4-Bromophenyl)-5-methyl-1H-1,2,3-triazol-4-yl)-3-(4-methoxyphenyl)prop-2-en-1-one (11b)

Yield (72.8%); mp: 235-237°C; IR (KBr, cm^{-1}): 3132 (CH, aromatic), 2960 (CH-aliphatic), 1700 (C=O); ^{1}H NMR (DMSO-d$_6$, δ ppm): 2.45 (s, 3H, CH$_3$), 3.82 (s, 3H, OCH$_3$), 7.02 (dd, 1H, --CO-CH=CH), 7.60-7.63 (m, 4H, Ar-H), 7.78 (dd, 1H, -CO-CH=CH), 7.81-7.86 (m, 4H, Ar-H); ^{13}C NMR (DMSO-d$_6$, δ ppm): 9.92 (CH3), 55.45 (OCH3), 114.64 (aromatic-C), 120.21 (-CO-CH=CH), 123.45, 126.99, 127.57, 130.74, 132.78, 134.34, 136.26, 138.99 (aromatic-C), 143.23 (-CO-CH=CH), 161.57 (aromatic-C), 183.30 (C=O); MS, m/z (%): 400 [M.$^+$+2] (27.35), 398 [M.$^+$] (24.95); Analysis for C$_{19}$H$_{16}$BrN$_3$O$_2$ (398.26), Calcd.: %C, 57.30; H, 4.05; N, 10.55. Found: %C, 57.48; H, 4.27; N, 10.72.

2.1.10.3. 1-(1-(4-Bromophenyl)-5-methyl-1H-1,2,3-triazol-4-yl)-3-(4-(dimethylamino) phenyl) prop-2-en-1-one (11c)

_____

Yield (65%); mp: 230-232°C; IR (KBr, cm^{-1}): 3132 (CH, aromatic), 2919 (CH-aliphatic), 1691 (C=O); ^{1}H NMR (DMSO-d_6, δ ppm): 2.59 (s, 3H, CH3), 3.02 (s, 6H, 2CH$_3$), 6.76 (dd, 1H, --CO-CH=CH), 7.64-7.66 (m, 4H, Ar-H), 7.76 (dd, 1H, -CO-CH=CH), 7.86-7.88 (m, 4H, Ar-H); ^{13}C NMR (DMSO-d_6, δ ppm): 10.30 (CH$_3$), 41.21 (2CH$_3$), 112.37, 117.30 (aromatic-C), 122.06 (-CO-CH=CH), 127.98, 131.12, 133.20, 134.86, 138.90, 143.91 (aromatic-C), 144.75 (-CO-CH=CH), 152.63 (aromatic-C), 183.51 (C=O); MS, m/z (%): 413 [M.$^{+}$+2] (15.29), 411 [M.$^{+}$] (16.47); Analysis for C$_{20}$H$_{19}$BrN$_4$O (411.30); Calcd.: %C, 58.40; H, 4.66; N, 13.62. Found: %C, 58.62; H, 4.71; N, 13.90.

2.1.10.4. 1-(1-(4-Bromophenyl)-5-methyl-1H-1,2,3-triazol-4-yl)-3-(3,4-dimethoxyphenyl)prop-2-en-1-one (11d)

Yield (73%); mp:165-167°C; IR (KBr, cm^{-1}): 3151 (CH, aromatic), 2999 (CH-aliphatic), 1695 (C=O); ^{1}H NMR (DMSO-d_6, δ ppm): 2.42 (s, 3H, CH3), 3.84 (s, 6H, 2OCH3), 6.78 (dd, 1H, -CO-CH=CH), 7.17-7.28 (m, 3H, Ar-H), 7.30-7.39 (m, 4H, Ar-H), 7.81 (dd, 1H, -CO-CH=CH); MS, m/z (%): 430 [M.$^{+}$+2] (22.74), 428 [M.$^{+}$] (24.51); Analysis for C$_{20}$H$_{18}$BrN$_3$O$_3$ (428.29); Calcd.: %C, 56.09; H, 4.24; N, 9.81; Found: %C, 56.31; H, 4.38; N, 10.05.

2.1.10.5. 3-(3-Bromo-4-hydroxy-5-methoxyphenyl)-1-(1-(4-bromophenyl)-5-methyl-1H-1,2,3-triazol-4-yl)prop-2-en-1-one (11e)

Yield (70%); mp: 185-187°C; IR (KBr, cm^{-1}): 3410 (OH), 3142 (CH, aromatic), 2919 (CH-aliphatic), 1682 (C=O); ^{1}H NMR (DMSO-d$_6$, δ ppm): 2.64 (s, 3H, CH3), 3.76 (s, 3H, OCH3), 7.04 (dd, 1H, CO-CH=CH), 7.40-7.46 (m, 2H, Ar-H), 7.60, 7.62 (2d, 4H, Ar-H), 7.85 (dd, 1H, -CO-CH=CH), 10.05 (s, 1H, OH, exchangeable with D$_2$O); ^{13}C NMR (DMSO-d$_6$, δ ppm): 10.12 (CH$_3$), 56.07 (OCH$_3$), 109.32 (aromatic-C), 123.65 (-CO-CH=CH), 127.95, 133.16, 134.68, 138.13, 138.39, 143.36, 144.28 (aromatic-C), 145.05 (-CO-CH=CH), 151.38 (aromatic-C), 182.61 (C=O); MS, m/z (%): 495 [M.$^{+}$+2] (20.37), 493 [M.$^{+}$] (22.06); Analysis for C$_{19}$H$_{15}$Br$_2$N$_3$O$_3$ (493.16), Calcd.: %C, 46.28; H, 3.07; N, 8.52. Found: %C, 46.37; H, 2.84; N, 8.73.

2.1.11. General procedure for the preparation of 4-(1-(4-bromophenyl)-5-methyl-1H-1,2,3-triazol-4-yl)-4H-sustituted pyrazole derivatives 12a,b.

A mixture of the chalcone derivatives 11c,e (30 mmol) and hydrazine hydrate 98% (3 mL, 90 mmol) in absolute ethanol was refluxed for 3 hrs. Upon cooling, white crystals were obtained, filtered, and crystallized from ethanol to obtain the corresponding compounds 12a,b.

2.1.11.1. 4-(3-(1-(4-Bromophenyl)-5-methyl-1H-1,2,3-triazol-4-yl)-1H-pyrazol-5-yl)-N,N-dimethylaniline (12a)

Yield (67%); mp: 167-169°C; IR (KBr, cm^{-1}): 3424 (NH), 3068 (CH, aromatic), 2917 (CH-aliphatic), 1595 (C=N); ^{1}H NMR (DMSO-d_6, δ ppm): 2.41, 2.86 (2s, 9H, 3CH$_3$), 6.68 (d, 2H, Ar-H), 7.18 (s, 1H, Pyrazole-H), 7.44 (s, 1H, NH, exchangeable with D$_2$O), 7.62-7.81 (m, 6H, Ar-H); ^{13}C NMR (DMSO-d_6, δ ppm): 9.92 (CH$_3$), 41.81 (-N(CH$_3$)$_2$), 110.11, 112.44, 122.80, 127.12, 127.22, 130.10, 131.63, 132.65, 134.96, 139.28, 143.41, 149.84, 155.31 (aromatic-C); MS, *m/z* (%): 425 [M.$^{+}$+2] (80.02), 423 [M^{+}] (77.73); Analysis for C$_{20}$H$_{19}$BrN$_6$ (423.32), Calcd.: %C, 56.75; H, 4.52; N, 19.85; Found: %C, 56.90; H, 4.68; N, 20.05.

2.1.11.2. 2-Bromo-4-(3-(1-(4-Bromophenyl)-5-methyl-1H-1,2,3-triazol-4-yl)-1H-pyrazol-5-yl)-6-methoxyphenol (12b)

Yield (69%); mp: 143-145°C; IR (KBr, cm^{-1}): 3530 (OH), 3420 (NH), 3100 (CH, aromatic), 2954 (CH-aliphatic), 1595 (C=N); ^{1}H NMR (DMSO-d_6, δ ppm): 2.41 (s, 3H, CH$_3$), 3.83 (s, 3H, OCH$_3$), 6.45 (s, 1H, Pyrazole-H), 7.02 (s, 1H, NH, exchangeable with D$_2$O), 7.56-7.66 (m, 4H, Ar-H), 7.81-7.85 (m, 2H, Ar-H), 9.50 (s, 1H, OH, exchangeable with D$_2$O). ^{13}C NMR (DMSO-d_6, δ ppm): 10.31 (CH$_3$), 56.61 (OCH$_3$), 109.45, 110.11, 121.65, 122.49, 125.58, 125.91, 127.58, 127.98, 130.19, 133.12, 139.53, 143.23, 148.87 (aromatic-C); MS, *m/z* (%): 507 [M.$^{+}$+2] (20.76), 505 [M.$^{+}$] (23.08); Analysis for C$_{19}$H$_{15}$Br$_2$N$_5$O$_2$ (505.17), Calcd.: %C, 45.17; H, 2.99; N, 13.86; Found: %C, 45.26; H, 3.27; N, 13.72.

2.1.12. General procedure for the preparation of 4-(3-(1-(4-bromophenyl)-5-methyl-1H-1,2,3-triazol-4-yl)-5-(4-(dimethylamino)phenyl)-1H-pyrazol-1-yl)-N-substituted benzene sulfonamide derivatives 13, 14.

Compound 13: A mixture of the chalcone derivatives 11b (3.90 g, 10 mmol) and 4-hydrazineyl-N-(pyrimidin-2-yl)benzenesulfonamide [47] (15 mmol) in glacial acetic acid (10 mL) was refluxed for 6 hrs. The mixture was poured into iced cubes and kept in refrigerator overnight. The separated product was filtered, and crystallized from ethanol to give the compound 13.

_____

Compound 14: A mixture of the chalcone derivatives **11c** (4.11 g, 10 mmol) and *N*-carbamimidoyl-4-hydrazineylbenzenesulfonamide [47] (15 mmol) in glacial acetic acid (10 mL) was refluxed for 6 hrs. The mixture was poured into iced cubes and kept in refrigerator overnight. The separated product was filtered, and crystallized from ethanol to give the compounds **14**.

2.1.12.1. 4-(3-(1-(4-Bromophenyl)-5-methyl-1*H*-1,2,3-triazol-4-yl)-5-(4-methoxyphenyl)-1*H*-pyrazol-1-yl)-*N*-(pyrimidin-2-yl)benzenesulfonamide (13)

Yield (74%); mp: 286-288°C; IR (KBr, cm^{-1}): 3324 (NH), 3059 (CH, aromatic), 2998 (CH-aliphatic), 1600 (C=N), 1313, 1171 (SO$_2$); ^{1}H NMR (DMSO-d_6, δ ppm): 2.60 (s, 3H, CH$_3$), 3.83 (s, 3H, OCH$_3$), 7.04 (m, 7H, Ar-H+ Pyrazole-H), 7.65-7.86 (m, 7H, Ar-H), 8.50 (m, 2H, Ar-H), 11.84 (s, 1H, NH, exchangeable with D$_2$O); ^{13}C NMR (DMSO-d_6, δ ppm): 10.33 (CH$_3$), 55.88 (OCH$_3$), 112.25, 115.09, 120.72, 121.07, 123.86, 125.64, 127.44, 127.98, 131.13, 133.21, 134.77, 136.83, 139.38, 143.66, 145.72, 153.87, 162.01, 163.72, 169.08; MS, *m/z* (%): 645 [M^{+}+2] (15.79), 643 [M.$^{+}$] (12.73); Analysis for C$_{29}$H$_{23}$BrN$_8$O$_3$S (643.52); Calcd.: %C, 54.13; H, 3.60; N, 17.41; S: 4.98. Found: %C, 53.92; H, 3.73; N, 17.58; S, 5.26.

2.1.12.2. 4-(3-(1-(4-Bromophenyl)-5-methyl-1*H*-1,2,3-triazol-4-yl)-5-(4-(dimethylamino) phenyl)-1*H*-pyrazol-1-yl)-*N*-carbamimidoylbenzenesulfonamide (14)

Yield (71.5%); mp: 290-292°C; IR (KBr, cm^{-1}): 3420, 4332 (NH$_2$, NH), 3100 (CH, aromatic), 2960 (CH-aliphatic), 1600 (C=N), 1313, 1171 (SO$_2$); ^{1}H NMR (DMSO-d_6, δ ppm): 2.19, 3.18 (2s, 9H, 3CH$_3$), 6.71 (s, 2H, NH$_2$, exchangeable with D$_2$O), 7.16-7.19 (m, 5H, Ar-H + pyrazole-H), 7.53-7.65 (m, 4H, Ar-H), 7.86-7.96 (m, 4H, Ar-H), 11.12, 11.26 (2s, 2H, 2NH, exchangeable with D$_2$O); MS, *m/z* (%): 622 [M^{+}+2] (18.38), 620 [M^{+}] (15.08); Analysis for C$_{27}$H$_{26}$BrN$_9$O$_2$S (620.53); Calcd.: %C, 52.26; H, 4.22; N, 20.32; S, 5.17; Found: %C, 52.38; H, 4.05; N, 20.52; S: 4.87.

2.2. Cytotoxic evaluation

2.2.1. Cell culture

The cell lines were purchased from the American Type Culture collection as follows: the breast carcinoma cell line (MCF-7) and the normal human diploid cell line (WI-38). Cytotoxic activity screening was performed using MTT assay [48,49] at Regional Center for Mycology and Biotechnology, Al- Azhar University. Exponentially, cells were placed in 10^4 cells/ well for 24 h, and then add fresh medium which containing different concentration of the tested sample. Serial two-fold dilutions of the tested sample were added using a multichannel pipette. Moreover, all cells were cultivated at 37 °C, 5% CO$_2$ and 95% humidity. Also, incubation of control cells occurred at 37 °C. However, after incubation for 24 h different concentrations of sample (50, 25, 12.5, 6.25, 3.125, 1.56 and 0 μg L^{-1}) were added and continued the incubation for 48 h, then, add the crystal violet solution 1% to each well for 0.5 h to examine viable cells. Rinse the wells using water until no stain. After that, add 30% glacial acetic acid to all wells with shaking plates on Microplate reader (TECAN, Inc.) to measure the absorbance, using a test wavelength of 490 nm. Besides, compare the treated samples with the control cell. The cytotoxicity was estimated by IC$_{50}$ in (μg /mL), the concentration that inhibits 50% of growth of cancer cell.

2.2.2. Aromatase inhibition assay

The aromatase inhibitory activity of the most active compounds was determined using a commercial fluorimetric assay (Aromatase CYP19A Inhibitor Screening kit, BioVision, Milpitas, CA, USA). The assay utilizes a fluorogenic aromatase substrate, that is converted into a highly fluorescent metabolite detected in the visible range (Ex/Em = 488/527 nm), ensuring a high signal-to-background ratio with little interference by autofluorescence. The inhibition assay and the IC$_{50}$ calculation were performed [50].

2.2.3. Molecular docking study

Compounds 5b, 5c, and 10 in addition to androstenedione (ASD) were built and structurally minimized using Schrödinger Maestro 12.8 [51]. Then, all the ligands were prepared for docking using AutoDock Tools 1.5.6 [52] through the addition of Gasteiger charges, merging the non-polar hydrogen, locating the aromatic carbons, detecting the rotatable bonds, and setting the torsions. The available human placental aromatase cytochrome P450 crystal structure (PDB ID: 3EQM) [53] through the protein data bank was downloaded and prepared for docking using AutoDock Tools 1.5.6. Water molecules were removed, hydrogens were added, non-polar hydrogens were merged, and Gasteiger charges were calculated. The grid box was adjusted using the same software with the x, y, z size of 40*40*40 Å, the spacing of 1 Å, and the x, y, z centers of 85.639, 54.467, and 45.921, respectively. Molecular docking of ASD and each individual ligand was then carried out using AutoDock Vina [54] and the exhaustiveness value of 20. Docking validation was first performed through comparing the prepared and docked ASD to the co-crystallized one in the active site of the aromatase cytochrome P450 enzyme. The
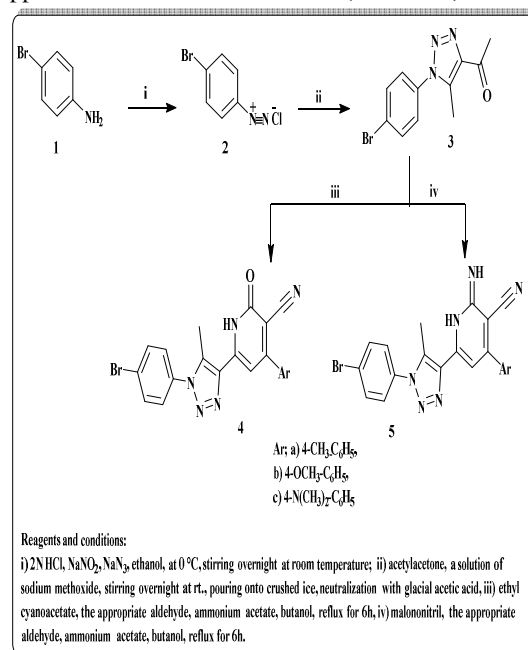
root mean square deviation (RMSD) was calculated using UCSF Chimera 1.15 [55]. After that, each ligand was docked using the same docking parameters. Finally, the docking results were analyzed using both UCSF Chimera 1.15 and AutoDock Tools 1.5.6 and all figures were prepared using UCSF Chimera 1.15.

3. Results and discussion
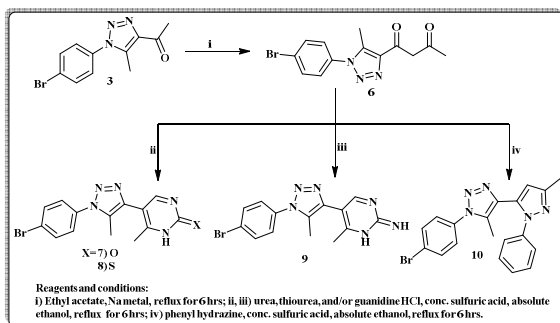### 3.1. Chemistry

The syntheses of the target 4-bromophenyl-5-methyl-1H-1,2,3-triazole derivatives **4–14** are depicted in **Schemes 1-3**. The key intermediate compound 1-(1-(4-bromophenyl)-5-methyl-1H-1,2,3-triazol-4-yl)ethan-1-one (**3**) prepared according to the reported method (44, 45) was treated with ethyl cyanoacetate and the appropriate aldehydes, namely p-tolyl, p-methoxy, and N,N dimethylamino benzaldehyes, in the presence of ammonium acetate to give the corresponding 2-oxo-1,2-dihydropyridine-3-carbonitrile derivatives **4a–c**. The IR spectra of the latter derivatives **4a–c** were characterized by the absorption bands at the regions 3425–3435, 2213–2217, and 1650 cm^{-1} assigned to the functional groups NH, CN, and C=O, respectively. ^{1}H NMR spectra of compounds **4a–c** were characterized by the appearance of a singlet signal at δ 2.29–2.40 ppm due to the 5-CH$_3$ protons, doublet and multiplet signals at the range δ 7.13–7.90 related to the aromatic protons, whereas the pyridine–H$_3$ appeared as a singlet signal at δ 6.70–6.80 ppm, whereas the NH proton appeared as a D$_2$O exchangeable singlet signal at δ 8.35-12.60 ppm. Moreover, additional singlet signals were recognized at δ 2.63, 3.83, and 3.02 ppm, assignable to 4-C$\underline{H}_3$-ph, 4-OC$\underline{H}_3$-ph, and 4-N(CH$_3$)$_2$-ph, respectively. The ^{13}C NMR spectrum of compound **4b** represented singlet signals at δ 10.75, 55.86 related to CH$_3$ and OCH$_3$, respectively, 114.76-155.09 due to the aromatic-C, and at δ 160.38 due to the C=O group. On the other hand, the reaction of the acetyl derivative **3** with malononitrile, and the appropriate aldehydes, namely *p*-tolyl, *p*-methoxy, and *N,N*-dimethylamino benzaldehydes, produced the corresponding 2-imino-4-1,2-dihydropyridine-3-carbonitriles **5a–c**. The IR spectra of the derivatives **5a–c** represented different absorption bands at 3433–4322 and 2207–2200 cm^{-1} related to the NH and CN functional groups. ^{1}H NMR spectra of compounds **5a-c** revealed singlet signals at δ 2.62, 3.83, and 3.01 assignable to 4-C$\underline{H}_3$-ph, 4-OC$\underline{H}_3$-ph, and -N(C$\underline{H}_3$)$_2$, respectively, and two D$_2$O exchangeable singlets at δ 8.30–10.26 ppm due to 2NH groups, in addition to the signals of the parent protons, which appeared at their expected regions. The ^{13}C NMR spectrum of compound **5b** exhibited signals at δ 10.06 and 56.58 ppm due to CH$_3$ and OCH$_3$ groups, respectively, as

well as different singlet signals at δ 116.02-154.87 ppm due to the aromatic carbons (**Scheme 1**).

Scheme 1: Synthesis of new 1,2,3-triazole -2-oxo-1,2-dihydropyridine and 1,2,3-triazole-2-imino-1,2-dihydropyridine derivatives **4a-c** and **5a-c**, respectively

Furthermore, the acetyl triazole derivative **3** was treated with ethyl acetate in the presence of Na metal to produce the corresponding diketone derivative **6**. The IR spectrum of the latter compound showed two characteristic bands at 1721 and 1684 cm^{-1} related to 2C=O groups. Also, the ^{1}H NMR spectrum of **6** represented two additional singlets at δ 2.40 and 3.87 ppm related to the methyl and the methylene protons of the diketone side chain alongside the signals of the parent scaffold, which appeared at their expected regions. The cyclization of the key acetyl derivative **3** was carried out with urea, thiourea, and guanidine in absolute ethanol in the presence of conc. sulfuric acid, leading to the formation of the corresponding 6-methylpyrimidine derivatives **7-9**, whereas its cyclization with phenyl hydrazine afforded the corresponding 3-methyl-1-phenyl-1*H*-pyrazole derivative **10**. The IR spectra of compounds **7-9** represented absorption bands at 3320-3327, 1678, 1200 related to NH, C=O and C=S groups, respectively. Also, the ^{1}H NMR spectra compounds **7-10** represented the appearance of a new singlet signal at δ 2.29 -2.39 ppm attributed to the pyrimidine-CH$_3$ and pyrazole-CH$_3$ protons besides the parent protons at their expected ranges. The ^{13}C NMR spectrum of compound **10** represented the pyrazole-$\underline{C}$H$_3$ at δ 13.77 ppm, while 1,2,3-triazole-$\underline{C}$H$_3$ appeared at δ 9.31 ppm (**Scheme 2**).
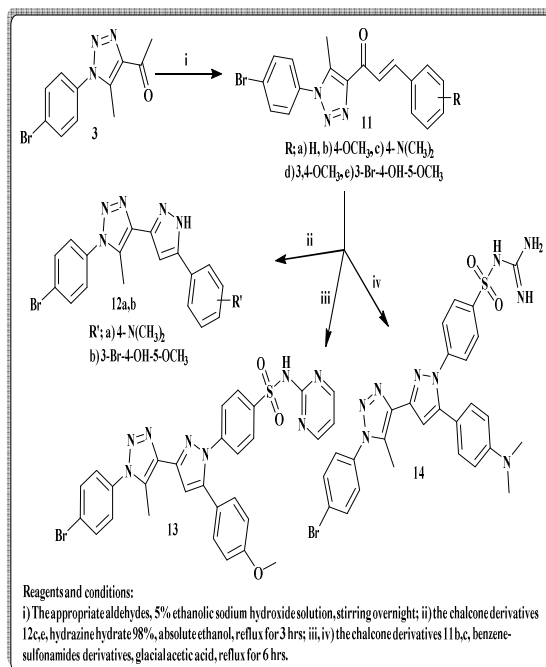
Scheme 2: Synthesis of the target 1,2,3-triazole-pyrimidine and 1,2,3-triazole-pyrazole derivatives **7-9** and **10**, respectively

Aldol condensation of the acetyl triazole derivative **3** with benzaldehyde and/or substituted benzaldehydes in an ethanolic sodium hydroxide solution led to the formation of the chalcone derivatives **11a–e**. The IR spectra of the chalcone derivatives exhibited absorption bands in the region 1700–1682 cm^{-1}, assignable to the C=O groups. ^{1}H NMR spectra of **11a-e** showed the two olefinic chalcone protons as two doublets at δ 6.76-7.90 ppm (J = 16.15 Hz). In addition, the ^{1}H NMR spectra of **11b,d** revealed the appearance of singlet signals at δ 3.82–3.84 ppm attributed to the OCH$_3$ moieties. while that of **11c** displayed a singlet signal integrating six protons at δ 3.02 ppm, proving the presence of the N(CH$_3$)$_2$ functional group. The ^{1}H NMR analysis of **11e** showed the OCH$_3$ moiety as a singlet signal at δ 3.76 ppm and the OH group as a D$_2$O exchangeable signal at δ 10.40 ppm. The protons of the parent molecules appeared in their correct positions **(Scheme 2)**.

Moreover, the chalcone derivatives **11c** and **11e** were allowed to condense with phenyl hydrazine in absolute ethanol to obtain the corresponding pyrazole derivatives **12a,b**. The presence of absorption bands around 3530 and 3424 cm^{-1} due to OH and NH groups was represented by the IR spectra of **12a,b**. The ^{1}H NMR spectra of both compounds **12a** and **12b** revealed, in addition to the parent signals, a singlet signal at δ 2.86 ppm integrated for six protons of the N(CH$_3$)$_2$ group (in the case of **12a**), a singlet signal at δ 3.83 ppm integrated for three protons of the OCH$_3$ group (in the case of **12b**), a third singlet at the region δ 6.45-7.18 ppm related to the Pyrazole-H, as well as D$_2$O exchangeable signals at δ 4.02-7.44, 9.50 ppm due to the NH and OH groups, respectively. The treatment of **11b** with sulfa pyrimidine and **11c** with 4-hydrazineyl-*N*-(pyrimidin-2-yl and / or (carbamimidoyl)benzenesulfonamides led to the formation of the corresponding benzenesulfonamide derivatives **13**, **14**. The IR spectra of **13**, **14** showed absorption bands around 3420, 4332, 1313, and 1171 cm^{-1} due to NH$_2$, NH and SO$_2$ functional groups. ^{1}H NMR spectra of the latter compounds showed D$_2$O

exchangeable singlets with chemical shifts at δ 11.84 ppm for compound **13** due to NH group and at δ 6.71, 11.12, and 11.26 ppm related to NH$_2$ and NH groups of compound **14**. The increase in the integration values in the down field chemical shift at δ 7.04 -8.50 ppm indicated the increase in the protons number related to the newly conjugated substituted benzenesulfonamide moiety of both **13** and **14**. ^{13}C NMR spectrum of compound **13** confirmed its structural formula **(Scheme 3)**.

The mass spectra of the new compounds exhibited molecular ion peaks that were in agreement with their molecular formulae

Scheme 3: Synthetic approaches of the target 1,2,3-triazole-pyrazole compounds **12a,b** and 1,2,3-triazole-pyrazole-benzenesulfonamide derivatives **13**, **14**

3.2. Biological activity
3.2.1. *In vitro* cytotoxic evaluation on human MCF-7 breast cancer cells

The compounds **4–14** were screened for their cytotoxic impact against human breast adenocarcinoma (MCF-7). 5-Fluorouracil was utilized as a positive control for comparison, and the viability of the cells was measured via the MTT colorimetric assay [51,52]. The obtained data are summarized in **Table 1**. Inspection of the obtained results demonstrated that the 2-iminopyridine congeners **5b** and **5c** elicited the most promising antiproliferative activity in comparison with 5-fluorouracil. The dimethylamino phenyl-2-imino-pyridine derivative **5c** appeared to be 1.4 times more potent than the reference drug, with IC$_{50}$ values of

3.9±2.3 and 5.6±0.89 µM, respectively. In addition, the cytotoxic activity of the other analogue, *p*-methoxyphenyl-2-imino-pyridine **5b,** was comparable to that of 5-fluorouracil, with an IC$_{50}$ value of 5.2± 2.1 µM. The third *p*-tolyl analogue, **5a**, on the other hand, showed a significant decrease in potency, with an IC$_{50}$ value of 74.5 4.0 µM. The conjugation of 4-methoxyphenyl and 4-*N,N*-dimethylaminophenyl to the parent 1,2,3-triazole scaffold might produce an extra hydrogen binding interaction with the amino acid residues of the target aromatase enzyme via oxygen and nitrogen atoms. Furthermore, MCF-7 cancer cells produced a sensitivity against the pyrazole derivative **10** similar to that against the reference drug (IC$_{50}$; 5.8±5.0 µM). The rest of the synthesized compounds appeared to be weak or inactive cytotoxic agents.

The frequency and severity of side effects in normal cells at therapeutic concentrations is one of the factors that distinguish different treatments from one another. Studying the safety profiles of the most potent compounds, **5b, c**, and **10**, against the normal human diploid cell line (WI-38), was therefore interesting. MTT assay was used to determine the suppression activity of the most potent compounds **5b, c**, and **10** against normal cells (**Table 1**). It was found that the tested derivatives **5b**, **c**, and **10** exhibited IC$_{50}$ values > 100, and 67.1 µM, respectively. The obtained results demonstrated promising safety margin of the tested compounds against normal cells.

Table 1
Growth inhibitory activity (IC$_{50}$; µM) of the newly synthesized compounds

Compounds	MCF-7 IC$_{50}$ (µM)	WI-38 IC$_{50}$ (µM)	SI
4a	41.2±5.1		
4b	41.8±2.3		
4c	29.3±2.3		
5a	74.5±4.0		
5b	5.2±2.1	> 100	> 1
5c	3.9±2.3	> 100	> 1
7	> 100		
8	> 100		
9	74.5±4.0		
10	5.8±5.0	67.1	11.6
11a	82.4±5.4		
11b	> 100		
11c	41.2±5.1		
11d	> 100		
11e	33.1±2.6		
12a	71.9±3.8		
12b	> 100		
13	> 100		
14	> 100		
5-FU	5.6±0.89		> 1

***3.2.2. In vitro* aromatase inhibition assay**

The strongest compounds, 5b, 5c, and 10, were tested using the *in vitro* fluorescence-based assay (Aromatase (CYP19A) Inhibitor Screening Kit (Fluorimetric) BioVision) to determine their potency to suppress the human aromatase enzyme. The fluorogenic substrate used in this experiment is transformed into a highly fluorescent metabolite that can be seen in the visible spectrum (Ex/Em = 488/527 nm) [17]. The results were contrasted with ketoconazole as a reference drug. Concentration-response curves for the tested compounds were derived in the *in vitro* fluorimetric assay and their IC$_{50}$ values for the aromatase inhibition were calculated. It can be detected that the most promising suppression effect was gained by compound 5b with an IC$_{50}$ value of 12.47 µM, in comparison with the reference drug ketoconazole with an IC$_{50}$ of 5.38 µM. The inhibitory activity was remarkably decreased by both compounds 5c and 10, with IC$_{50}$ values of 35.43 and 25.48 µM, respectively (Fig. 3).

The promising anticancer activity of the tested compounds 5b, 5c, and 11a could be related to other mechanisms of action in addition to aromatase inhibitory effect (Fig. 4).

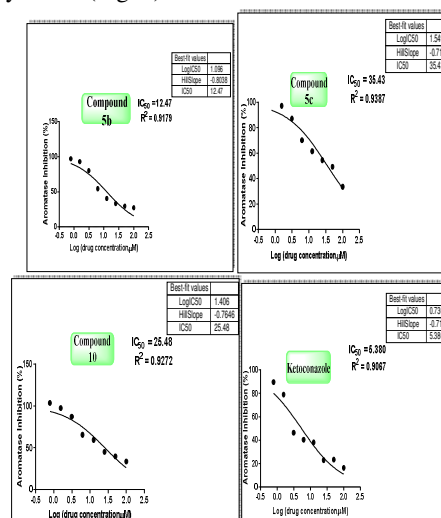**Fig. 4:** The aromatase suppression activities of the compounds 5b, 5c, and 10 in comparison with ketoconazole

4. Molecular docking studies

Molecular docking was performed for compounds **5b**, **5c**, and **10** against the crystal structure of the human placental aromatase cytochrome P450 enzyme (PDB ID: 3EQM) [52]. The grid box was adjusted to surround the active site of the enzyme as well as two potential allosteric sites that have been previously reported for the design of allosteric modulators [56-58]. Molecular docking of androstenedione (**ASD**) was first performed against the enzyme to validate

the selected docking parameters before running the docking of the three ligands. An excellent RMSD value of 0.4 Å was calculated for the docked **ASD** in comparison to the co-crystallized one in the active site of the enzyme. The docked pose of **ASD** possessed a binding energy of -13.7 kcal/mol and a similar hydrogen bond between its C=O group and the backbone NH of MET374 to that between the co-crystallized **ASD** molecule and the same residue (**Fig. 5**). Thus, the same parameters were employed for docking all the individual ligands against the enzyme. Molecular docking results of the pose with the lowest binding energy of each compound are illustrated in **Table 2**.

The docking results of compounds **5b** and **5c** did not prove binding affinity to the active site of the enzyme. However, they showed good binding affinity to another site that has been previously reported by Magistrato and colleague researchers [56-58] as one of potential allosteric sites in the enzyme for which allosteric modulators could be designed to target the enzyme while reducing the side effects caused by drugs that bind to the active site.

In the potential allosteric site 1, compounds **5b** and **5c** exhibited the same binding energy of -8.1 kcal/mol and very similar binding modes as well (**Fig. 5**). The two ligands possessed two hydrogen bonds with site 1 residues, the first hydrogen bond between their nitrile N and the NH_2 of GLN218, while the second hydrogen bond between their triazole N and the NH_2 of GLN225. Compound **5b** possessed an additional hydrogen bond between its methoxy O and the NH_2 of ARG192.

The binding mode of compound **10** to the allosteric site 2 involved the binding energy of -8.3 kcal/mol and the formation of three hydrogen bonds between the triazole N of the compound and both the NH_2 of GLN428 and the NH_3^+ of LYS440. Significant π-π interactions were also located between the phenyl and triazole rings of compound **10** and the phenyl ring of TYR424, and between the pyrazole ring of the compound and the phenyl ring of TYR441 (**Fig. 5, Table 2**).

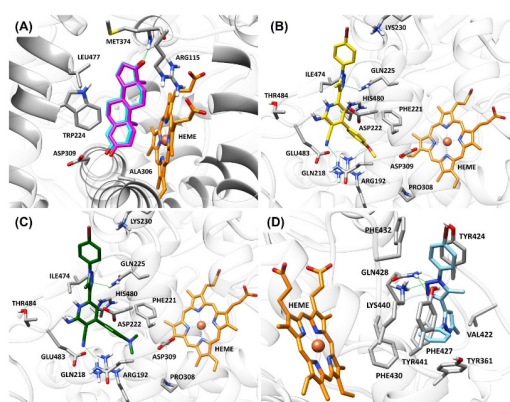**Fig. 5:** Ligands bound to human placental aromatase cytochrome P450 (PDB ID: 3EQM) [52]. (**A**) Docking validation results with an RMSD value of 0.4 Å between the docked **ASD** (shown in magenta) and the co-crystallized **ASD** (shown in cyan) in the active site of the enzyme. (**B**) Docked pose of compound **5b** in the potential allosteric site 1. (**C**) Docked pose of compound **5c** in the same allosteric site 1. (**D**) Docked pose of compound **10** in the potential allosteric site 2. Protein and residues are shown in gray; heme moiety is displayed in orange, while hydrogen bonds are depicted as green lines.

Table 2

Molecular docking results against human placental aromatase cytochrome P450

Ligand	Binding Site	Binding Energy (kcal/mol)	Number of Hydrogen Bonds	Groups forming Hydrogen Bonds	
				Ligand	Residue
ASD	Active Site	-13.7	1	C=O	MET374 NH
5b	Allosteric Site 1	-8.1	3	CH_3O $C≡N$ Triazole N	ARG192 NH_2 GLN218 NH_2 GLN225 NH_2
5c	Allosteric Site 1	-8.1	2	$C≡N$ Triazole N	GLN218 NH_2 GLN225 NH_2
10	Allosteric Site 2	-8.3	3	Triazole N Triazole N Triazole N	GLN428 NH_2 GLN428 NH_2 LYS440 NH_3^+

5. Conclusions

In summary, a series of compounds bearing 4-bromophenyl-5-methyl-1,2,3-triazole scaffold hybridized with various heterocyclic ring systems such as pyridine, pyrimidine, and pyrazole **4-14** have been synthesized and evaluated as cytotoxic agents against breast cancer cell (MCF-7). The 2-iminopyridine molecules **5b** and **5c** and the pyrazole derivative **10** revealed the most promising antiproliferative activity in comparison with 5-fluorouracil (IC_{50}; 5.2± 2.1, 3.9±2.3, 5.8±5.0, 5.6±0.89 µM, respectively). Moreover, the latter analogues exhibited a high safety margin against the human normal (WI38). In addition, the compounds **5b**, **5c** and **10** were further subjected to aromatase inhibitory activity using ketoconazole as a reference drug. The 4-methoxy derivative **5b** represented the most promising aromatase suppression activity in comparison with ketoconazole (IC_{50}; 12.47 µM, IC_{50} ketoconazole; 5.38 µM). Less inhibitory potency was detected by the other two derivatives **5c** and **10** (IC_{50}; 35.43 and 25.48 µM, respectively).

Molecular docking study was performed for the compounds **5b**, **5c**, and **10** to find out their modes of interactions with aromatase enzyme. More molecular modification and optimization is required for 1,2,3-

_____

triazole derivatives to enhance their inhibitory activity against aromatase enzyme resulting in more potent antiproliferative activity against breast cancer.

6. Acknowledgements

7. Conflicts of interest

There are no conflicts of interest.

8. References

1. Rashdan H.R., Shehadi I.A. Triazoles synthesis & applications as nonsteroidal aromatase inhibitors for hormone-dependent breast cancer treatment. *heteroat. chem.* **2022** (2022).

2. Desantis C.E., Ma J., Gaudet M.M., Newman L.A., Miller K.D., Sauer A.G., Jemal A., Siegel, R.L. Breast Cancer Statistics. *CA Cancer J. Clin.* **69**, 438-451 (2019).

3. Adhikari N., Amin S.A., Saha A., Jha T. Combating breast cancer with nonsteroidal aromatase inhibitors (NSAIs): Understanding the chemico-biological interactions through comparative SAR/QSAR study. *Eur. J. Med. Chem.* **137**, 365–438 (2017).

4. Waks A.G., Winer E.P. Breast cancer treatment: a review. *Jama.* **321**, 288–300 (2019).

5. Pistelli M., Mora A.D., Ballatore Z., Berardi R. Aromatase inhibitors in premenopausal women with breast cancer: the state of the art and future prospects. *Curr. Oncol.* 25, e168–e175 (2018).

6. Chen K.L., Madak-Erdogan Z. Estrogens and female liver health. *Steroids.* **133**, 38–43. (2018).

7. Lim E., Metzger-Filho O., Winer E.P. The natural history of hormone receptor-positive breast cancer. *Oncology.* **26**, 688–696 (2012).

8. Hetemaki N., Savolainen-Peltonen H., Tikkanen M.J., Wang F., Paatela H., Hamalainen E., Turpeinen U., Haanpaa M., Vihma V., Mikkola T.S. Estrogen metabolism in abdominal subcutaneous and visceral adipose tissue in postmenopausal women. *J. Clin. Endocrinol. Metab.* **102**, 4588–4595 (2017).

9. Hetemäki N., Mikkola T.S., Tikkanen M.J., Wang F., Hämäläinen E., Turpeinen U., Haanpää M., Vihma V., Savolainen-Peltonen H. Adipose tissue estrogen production and metabolism in premenopausal women. *J. Steroid Biochem. Mol. Biol.* **209**, 105849 (2021).

10. Jiang C.F., Shi Z.M., Li D.M., Qian Y.C., Ren Y., Bai X.M., Xie Y.X., Wang L., Ge, X., Estrogen-induced miR-196a elevation promotes tumor growth and metastasis via targeting SPRED1 in breast cancer. Mol Cancer 17, 83 (2018).

11. Liu W.T., Zhen L.L., Liu L.Z., Jiang B.H. Estrogen-induced miR-196a elevation promotes tumor growth and metastasis via targeting SPRED1 in breast cancer. *Mol. Cancer.* **17**, 1–8 (2018).

12. Thomas C., Gustafsson J.A. The different roles of ER subtypes in cancer biology and therapy. Nat. Rev. *Cancer.* **11**, 597–608 (2011).

13. Yasar P., Ayaz G., User S.D., Gupur G., Muyan M. Molecular mechanism of estrogen–estrogen receptor signaling. *Reprod. Med. Biol.* **16**, 4–20 (2017).

14. Karkola S., Holtje H.D., Wahala K. A three-dimensional model of CYP19 aromatase for structure-based drug design. J. Steroid Biochem. *Mol. Biol.* **105**, 63–70 (2007).

15. Ghosh D., Lo J., Egbuta, C. Recent progress in the discovery of next generation inhibitors of aromatase from the structure-function perspective. *J. Med. Chem.* **59**, 5131–5148 (2016).

16. Sychev D.A., Ashraf G.M., Svistunov A.A., Maksimov M.L., Tarasov V.V., Chubarev V.N., Otdelenov V.A., Denisenko N.P., Barreto G.E., Aliev G. The cytochrome P450 isoenzyme and some new opportunities for the prediction of negative drug interaction *in vivo*. *Drug Des. Devel. Ther.* **12**, 1147–1156 (2018).

17. Stocco, C. Tissue physiology and pathology of aromatase. *Steroids.* **77**, 27–35 (2012).

18. Ammazzalorso A., Gallorini M., Fantacuzzi M., Gambacorta N., De Filippis B., Giampietro L., Maccallini C., Nicolotti O., Cataldi A., Amoroso R. Design, synthesis and biological evaluation of imidazole and triazole-based carbamates as novel aromatase inhibitors. *Eur. J. Med. Chem.* **211**, 113115 (2021).

19. Favia A.D., Nicolotti O., Stefanachi A., Leonetti F., Carotti A. Computational methods for the design of potent aromatase inhibitors. *Expert Opin. Drug Discov.* **8**, 395 (2013).

20. Brown K. Breast cancer chemoprevention: risk-benefit effects of the antioestrogen tamoxifen. *Expert Opin. Drug Saf.* **1(3)**, 253-67 (2002).

21. Benz C.C., Scott G.K., Sarup J.C., Johnson R.M., Tripathy D., Coronado E., Shepard H.M., Osborne C.K. Estrogen-dependent, tamoxifen-

_____

resistant tumorigenic growth of MCF-7 cells transfected with HER2/neu. *Breast Cancer Res. Treat.* **24**, 85-95 (1993).

22. Jordan V.C. Selective estrogen receptor modulation: concept and consequences in cancer. *Cancer Cell.* **5**, 207-213 (2004).

23. Brueggemeier R.W., Hackett J.C., Diaz-Cruz E.S. Aromatase inhibitors in the treatment of breast cancer. *Endocr. Rev.* **26**, 331-345 (2005).

24. Sainsbury R. The development of endocrine therapy for women with breast cancer. *Cancer. Treat Rev.* **39**, 507-517 (2013).

25. Ahmad Shagufta I. Recent developments in steroidal and nonsteroidal aromatase inhibitors for the chemoprevention of estrogen-dependent breast cancer. *Eur. J. Med. Chem.* **102**, 375-386 (2015).

26. Avvaru S.P., Noolvi M.N., Aminbhavi T.M., Chkraborty S., Dash A., Shukla, S.S. Aromatase inhibitors evolution as potential class of drugs in the treatment of postmenopausal breast cancer women. *Mini Rev. Med. Chem.* **18**, 609-621 (2018).

27. Cocconi G. First generation aromatase inhibitors aminoglutethimide and testololactone. *Breast Cancer Res. Treat.* **30**, 57–80 (1994).

28. Ghosh D., Lo J., Egbuta C. Recent progress in the discovery of next generation inhibitors of aromatase from the structure–function perspective. *J med chem.* **59(11)**, 5131-5148 (2016).

29. Thürlimann B., Keshaviah A., Coates A.S., Mouridsen H., Mauriac L., Forbes J.F., Paridaens R., Castiglione-Gertsch M., Gelber R.D., Rabaglio M., Smith I. Breast International Group (BIG) 1-98 Collaborative Group. A comparison of letrozole and tamoxifen in postmenopausal women with early breast cancer. *N. Engl. J. Med.* **353**, 2747-57 (2005).

30. Jakesz R., Jonat W., Gnant M., Mittlboeck M., Greil R., Tausch C., Hilfrich J., Kwasny W., Menzel C., Samonigg H., Seifert M. Switching of postmenopausal women with endocrine-responsive early breast cancer to anastrozole after 2 years' adjuvant tamoxifen: combined results of ABCSG trial 8 and ARNO 95 trial. *Lancet.* **366**, 455-462 (2005).

31. Chang W.T., Chen P.W., Lin, H.W., Kuo Y.H., Lin S.H., Li Y.H. Risks of Aromatase Inhibitor-Related Cardiotoxicity in Patients with Breast Cancer in Asia. *Cancers.* **14(3)**, 508 (2022).

32. Alam M.M. 1,2,3-Triazole hybrids as anticancer agents: A review. *Arch. Pharm.* **355**, e2100158 (2022).

33. Kumar R., Vats L., Bua S., Supuran C.T., Sharma P.K. Design and synthesis of novel benzenesulfonamide containing 1, 2, 3-triazoles as potent human carbonic anhydrase isoforms I, II, IV and IX inhibitors. *Eur. J. Med. Chem.* **155**, 545-51 (2018).

34. Baraniak D., Baranowski D., Ruszkowski P., Boryski J. Nucleoside dimers analogues with a 1, 2, 3-triazole linkage: Conjugation of floxuridine and thymidine provides novel tools for cancer treatment. Part II. *Nucleosides Nucleotides Nucleic Acids.* **38(11)**, 807-35 (2019).

35. Banerji B., Chandrasekhar K., Sreenath K., Roy S., Nag S., Saha K.D. Synthesis of triazole-substituted quinazoline hybrids for anticancer activity and a lead compound as the EGFR blocker and ROS inducer agent. *ACS omega.* **3(11)**, 16134-42 (2018).

36. Ghosh D., Lo J., Egbuta, C. Recent progress in the discovery of next generation inhibitors of aromatase from the structure-function perspective. *J. Med. Chem.* **59**, 5131-5148 (2016).

37. Thurlimann B., Keshaviah A., Coates A.S., Mouridsen H., Mauriac L., Forbes J.F., Paridaens M., Castiglione-Gertsch M., Gelber R.D., Rabaglio M., Smith I., Wardley A., Price K.N., Goldhirsch A. A comparison of letrozole and tamoxifen in postmenopausal women with early breast cancer. *N. Engl. J. Med.* **353**, 2747-2757 (2005).

38. Jakesz R., Jonet W., Gnant M., Mittleboeck M., Greil R., Tausch C., Hilfrich J., Kwasny W., Menzel C., Samonigg, H. Switching of postmenopausal women with endocrine responsive early breast cancer to anastrozole after 2 years' adjuvant tamoxifen: combined results of ABCSG trial 8 and ARNO 95 trial. *Lancet.* **366**, 455-462 (2005).

39. El-Naggar M., Abd El-All A.S., El-Naem S.I., Abdalla M.M., Rashdan H.R. New potent 5α-Reductase and aromatase inhibitors derived from 1, 2, 3-triazole derivative. *Molecules.* **25(3)**, 672 (2020).

40. Doiron J., Richard R., Touré M.M., Picot N., Richard R., Čuperlović-Culf M., Robichaud G.A., Touaibia M. Synthesis and structure–activity relationship of 1-and 2-substituted-1, 2, 3-triazole letrozole-based analogues as aromatase inhibitors. *Eur J. Med. Chem.* **46(9)**, 4010-24 (2011).

41. Pingaew R., Prachayasittikul V., Mandi P., Nantasenamat C., Prachayasittikul S., Ruchirawat S., Prachayasittikul V. Synthesis and molecular docking of 1, 2, 3-triazole-based sulfonamides as

aromatase inhibitors. *Bioorg Med. Chem.* **23(13)**, 3472-3480 (2015).

42. McNulty J., Nair J.J., Vurgun N., DiFrancesco B.R., Brown C.E., Tsoi B., Crankshaw D.J., Holloway A.C. Discovery of a novel class of aldol-derived 1, 2, 3-triazoles: Potent and selective inhibitors of human cytochrome P450 19A1 (aromatase). *Bioorg. Med Chem Lett.* **22(1)**, 718-22 (2012).

43. Ertas M., Sahin Z., Berk B., Yurttas L., Biltekin S.N., Demirayak S. Pyridine-substituted thiazolylphenol derivatives: Synthesis, modeling studies, aromatase inhibition, and antiproliferative activity evaluation. *Arch Pharm (Weinheim).* **351(3-4)**, e1700272 (2018).

44. Okada, M., Yoden, T., Kawaminami, E., Shimada, Y., Kudou, M., Isomura, Y. Studies on aromatase inhibitors IV. Synthesis and biological evaluation of N, N-Disubstituted-5-aminopyrimidine derivatives. *Chem. Pharm. Bull.* **45(8)**, 1293-1299 (1997).

45. Yi1 X-J., T. El-Idreesy T., Eldebss T.M. A., Farag A. M, Abdulla M.M., Hassan S.A., Mabkhot Y.N. Synthesis, biological evaluation, and molecular docking studies of new pyrazol-3-one derivatives with aromatase inhibition activities. *Chem Biol Drug Des.* **88**, 832–843 (2016).

46. Singh H., Sindhu J., Khurana J.M. Synthesis of biologically as well as industrially important 1, 4, 5-trisubstituted-1, 2, 3-triazoles using a highly efficient, green and recyclable DBU–H 2 O catalytic system. *RSC Advances.* **3(44)**, 22360-22366 (2013).

47. Winum J.Y., Dogné J.M., Casini A., de Leval X., Montero J.L, Scozzafava A., Vullo D., Innocenti A., Supuran C.T. Carbonic anhydrase inhibitors: synthesis and inhibition of cytosolic/membrane-associated carbonic anhydrase isozymes I, II, and IX with sulfonamides incorporating hydrazino moieties. *J. med. chem*. **48(6)**, 2121-2125 (2005).

48. Mosmann, T. Rapid colorimetric assay for cellular growth and survival: Application to proliferation and cytotoxicity assays. *J. Immunol. Methods.* **65**, 55–63 (1983).

49. Elaasser M.M., Morsi M.K., Galal S.M., El-Rahman M.K.A., Katry M.A. Antioxidant, anti-inflammatory and cytotoxic activities of the unsaponifiable fraction of extra virgin olive oil. *Grasas y Aceites*. **71**, 386 (2020).

50. Fantacuzzi M., De Filippis B., Gallorini M., Ammazzalorso A., Giampietro L., Maccallini C., Aturki Z., Donati E., Ibrahim R.S., Shawky E., Cataldi A., Amoroso, R. Synthesis, biological evaluation, and docking study of indole aryl sulfonamides as aromatase inhibitors. *Eur. J. Med. Chem.* **185**, 111815 (2020).

51. Schrödinger Release 2021-3: Maestro, Schrödinger, LLC, New York, NY, (2021).

52. Morris G.M., Huey R., Lindstrom W., Sanner M.F., Belew R.K., Goodsell D.S., Olson A.J. AutoDock4 and AutoDockTools4: Automated docking with selective receptor flexibility. *J. Comput. Chem.* **30(16)**, 2785-2791 (2009).

53. Ghosh D., Griswold J., Erman M., Pangborn W. Structural basis for androgen specificity and oestrogen synthesis in human aromatase. *Nature.* **457(7226)**, 219-223 (2009).

54. Trott O., Olson A.J. AutoDock Vina: improving the speed and accuracy of docking with a new scoring function, efficient optimization, and multithreading. *J. Comput. Chem.* **31(2)**, 455-461 (2010).

55. Pettersen E.F., Goddard T.D., Huang C.C., Couch G.S., Greenblatt, D.M., Meng E.C., Ferrin, TE. UCSF Chimera—a visualization system for exploratory research and analysis. *J. Comput. Chem.* **25(13)**, 1605-1612 (2004).

56. Spinello A., Martini S., Berti F., Pennati M., Pavlin M., Sgrignani J., Grazioso G., Colombo G., Zaffaroni N., Magistrato, A. Rational design of allosteric modulators of the aromatase enzyme: An unprecedented therapeutic strategy to fight breast cancer. *Eur. J. Med. Chem.* **168**, 253-262 (2019).

57. Magistrato A., Sgrignani J., Krause R., Cavalli A. Single or multiple access channels to the CYP450s active site? An answer from free energy simulations of the human aromatase enzyme. *J. Phys. Chem. Lett.* **8(9)**, 2036-2042 (2017)

58. Sgrignani J., Bon M., Colombo G., Magistrato A. Computational approaches elucidate the allosteric mechanism of human aromatase inhibition: a novel possible route to small-molecule regulation of CYP450s activities?. *J. Chem. Inf. Model.* **54(10)**, 2856-2868. (2014).